IEEE Access
Multidisciplinary | Rapid Review | Open Access Journal

Received April 22, 2022, accepted May 9, 2022, date of publication May 12, 2022, date of current version May 19, 2022.

Digital Object Identifier 10.1109/ACCESS.2022.3174695

Low-Profile and Wideband Circularly Polarized Magneto-Electric Dipole Antenna Excited by a Cross Slot

SON TRINH-VAN, YOUNGOO YANG, (Senior Member, IEEE), KANG-YOON LEE, (Senior Member, IEEE), AND KEUM CHEOL HWANG, (Senior Member, IEEE)
Department of Electrical and Computer Engineering, Sungkyunkwan University, Suwon 440-746, South Korea

Corresponding author: Keum Cheol Hwang (khwang@skku.edu)

This work was supported by the Institute of Information and Communications Technology Planning and Evaluation (IITP) Grant through the Korean Government Ministry of Science and Information and Communication Technologies—MSIT (Development of low power/low delay/self-power suppliable RF simultaneous information and power transfer system and stretchable electronic epineurium for wireless nerve bypass implementation) under Grant 2020-0-00261.

ABSTRACT In this article, we present the design of a low-profile circularly polarized (CP) magneto-electric (ME) dipole antenna with enhanced CP bandwidth properties. The ME dipole antenna is excited by a simple microstrip line aperture-coupled feeding structure. The coupling aperture is composed of two crossed slots of unequal lengths to realize CP operation. Four identical inverted L-shaped parasitic elements, each consisting of a horizontal patch and a vertical metallic plate, are vertically positioned around the ME dipole. It was found that such parasitic elements can remarkably improve the 3 dB axial ratio (AR) bandwidth while retaining the wide impedance bandwidth. A prototype with a low profile of only $0.134\lambda_L$ (λ_L is the wavelength in free space at the lowest operating frequency) is fabricated and tested to verify the proposed design. The experimental results show that the prototype has an overlapping impedance bandwidth ($|S_{11}| \leq -10$ dB) and a 3 dB AR bandwidth of 3.16–5.36 GHz (51.35%) with a maximum broadside left-handed CP gain of 9.75 dBic. Additionally, nearly identical radiation patterns on two principle cutting planes are obtained over the operating band.

INDEX TERMS Aperture-coupled, circularly polarized (CP) antenna, low profile, magneto-electric (ME) dipole, parasitic element, wideband.

I. INTRODUCTION

Since the magneto-electric (ME) dipole antenna was successfully implemented for the first time by Luk and Wong in 2006 [1], it has drawn significant attention from antenna researchers. The attention is warranted because the ME dipole antenna possesses the excellent features of a wide impedance bandwidth, a high gain, and especially nearly identical polarized E-and H-plane radiation patterns with low cross-polarization [2], [3]. Numerous ME dipole antennas have been demonstrated for variety of applications on both the microwave and millimeter-wave bands, including broadband/multiband designs [4], [5], linearly polarized (LP) designs [6]–[8], dual-polarized designs [9], [10], and circularly polarized (CP) designs [11]–[14], among others. Among these different types of antennas, CP antennas are preferred owing to their superior ability to reduce the detrimental influence of multi-path interference and mitigate the polarization mismatch between the transmitting and receiving antennas [15], [16]. Therefore, this has led to increased interest in developing the CP ME dipole antennas, as noted in various studies [11]–[14], [17]–[23].

Various CP ME dipole antennas have been reported in the literature [17]–[24]. In one study [17], by modifying the horizontal patches of a ME dipole antenna into a trapezoidal shape, a CP ME dipole antenna with a 3 dB AR bandwidth of 41% (1.7–2.6 GHz) was realized, but its profile was approximately $0.24\lambda_L$ (λ_L is the wavelength in free space at the lowest operating frequency). By adding strips that were bent downward to the ends of horizontal trapezoidal

The associate editor coordinating the review of this manuscript and approving it for publication was Giorgio Montisci.

patches and introducing a cavity reflector with four gaps, a CP ME dipole antenna with a low profile of $0.16\lambda_L$ was developed [18], reportedly achieving a wide 3 dB AR bandwidth of 79.7% (1.6–3.72 GHz). A CP ME dipole antenna with a wide 3 dB AR bandwidth of 67.2% and a low profile of $0.177\lambda_L$ was presented by adding vertically shorted plates to the outside edges of the horizontal planar electric dipole [19]. These CP ME antennas in all cases were excited by a suspended Γ-shaped probe. Recently, a type of CP ME dipole antenna with a microstrip line aperture-coupled excitation was also introduced. Compared to the suspended Γ-shaped probe, the microstrip line aperture-coupled excitation structure is much simpler and easier to fabricate. In other work [20], a slot-coupled fed CP ME dipole antenna with a very high profile of $0.287\lambda_L$ was introduced and a 3 dB AR bandwidth of 22.5% (3.75–4.70 GHz) was achieved by connecting two horizontal planar patches at the diagonal position. In another design [21], by employing a single-series feeding cross-aperture coupled structure, a CP ME dipole with a low profile of $0.166\lambda_L$ was presented, reaching a 3 dB AR bandwidth of 23.5% (4.98–6.31 GHz). A CP bandwidth up to 64.5% (2.7–5.8 GHz) was developed in a cross-aperture coupled CP ME dipole antenna with a profile of $0.168\lambda_L$ by integrating with a wideband feeding network [22]. In recent work [23], a CP ME dipole antenna with a low profile of only $0.122\lambda_L$ fed by substrate integrated waveguide aperture-coupled feeding structure with a butterfly-shaped slot was reported. However, this antenna exhibited a very narrow 3 dB AR bandwidth of only 12.8% (22.6–25.7 GHz). Clearly, designing a CP ME dipole antenna with a low-profile structure and a broad 3 dB AR bandwidth simultaneously is very challenging.

In this paper, a low-profile and broadband CP ME dipole antenna with microstrip line aperture-coupled excitation is proposed. The coupling aperture is composed of two crossed slots etched on the ground plane. The lengths of these two slots are unequal to realize CP operation. Then, by introducing four identical parasitic inverted *L*-shaped patches around the ME dipole antenna, an increase of nearly six-fold in the 3 dB AR bandwidth can be achieved. The performance of the proposed CP ME dipole antenna is basically analyzed and optimized with the help of the ANSYS HFSS full-wave simulator and is experimentally verified through a fabricated prototype. The experimental results are in good agreement with the simulated ones. The fabricated prototype has a low profile of only $0.134\lambda_L$, an overlapping 3 dB AR/impedance bandwidth of 51.35% from 3.16 to 5.36 GHz, and a broadside left-handed CP gain from 5.50 to 9.75 dBic. Additionally, the radiation patterns on the two principle cutting planes are nearly identical over the operating band.

The organization of this paper is as follows. Section II presents the antenna configuration, design procedure, operating principle, and the results of a parameter study of the proposed design. In Section III, the experimental results of the fabricated prototype are summarized and described. Finally, Section IV provides the conclusion.

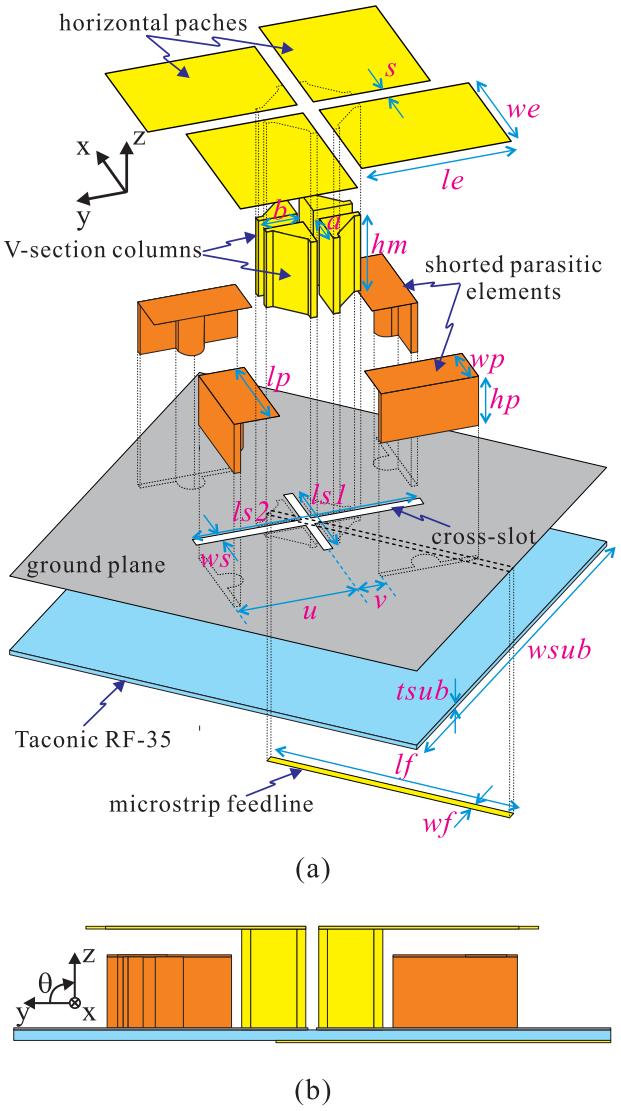

FIGURE 1. Geometry of the proposed CP ME dipole antenna. (a) Perspective view. (b) Side view).

II. ANTENNA DESIGN

A. ANTENNA CONFIGURATION

Figure 1 presents an illustration of the geometry and detailed dimensions of the proposed CP ME dipole antenna with a microstrip line aperture-coupled excitation. The antenna mainly consists of three parts. The first part is a ME dipole, which is composed of four identical horizontal planar patches and four V-section columns arranged in a sequentially rotated structure. The horizontal planar patches are attached at the top of the V-section columns, which are positioned normal to the ground plane. They together form two pairs of electric dipoles along the *x*-axis and *y*-axis. The V-section columns and the ground plane form two crossed magnetic dipoles along the *x*-axis and *y*-axis, respectively. The second part of the antenna consists of four identical parasitic inverted *L*-shaped shorted patches, which are also arranged in a sequentially rotated structure around the ME dipole. Each parasitic element consists of a horizontal patch and a vertically shorted plate.

TABLE 1. Geometrical dimensions of the proposed CP ME dipole antenna.

Parameter	we	le	s	a	b
Value/mm	18	23	2.5	6	6
Parameter	hm	hp	lp	wp	ws
Value/mm	11.2	9.2	15	7	0.725
Parameter	$ls1$	$ls2$	u	v	$tsub$
Value/mm	35	17	18.5	4.5	0.508
Parameter	$wsub$	lf	wf		
Value/mm	65	38.75	0.8		

The third part of the antenna is a square printed circuit board with a width of *wsub*. This substrate is a Taconic RF-35 with a thickness of *tsub*, a dielectric constant of 3.5, and a loss tangent of 0.0018. The top surface of the substrate is the ground plane. A 50-Ω microstrip feedline is printed on the bottom surface of the substrate. Two crossed slots of unequal lengths are etched on the ground plane at the center. As a result, a microstrip line aperture-coupled excitation mechanism is formed to feed the ME dipole. Compared to the conventional Γ-shaped probe, the microstrip line aperture-coupled excitation method is much easier in terms of fabrication. The geometrical design parameters of the proposed CP ME dipole antenna are optimized to maximize the overlapping 3 dB AR/impedance bandwidth (determined by the criteria of $|S_{11}| \leq -10$ dB and AR ≤ 3 dB). The optimized design parameters are summarized in Table 1.

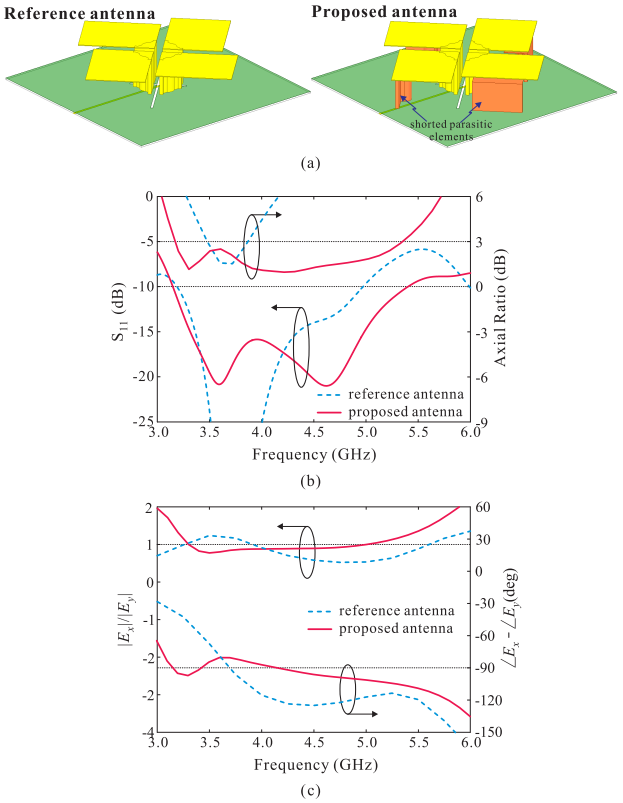

FIGURE 2. (a) Design process of the proposed CP ME dipole antenna. (b) Simulated reflection coefficients and ARs. (c) Simulated amplitude ratios and phase differences of the orthogonal electric far-fields.

B. OPERATING MECHANISM

Figure 2(a) shows the design process of the proposed CP ME dipole antenna. Based on the design of a LP ME dipole antenna [24], we initially developed a CP ME dipole antenna fed by a microstrip line aperture-coupled excitation method (reference antenna). The coupling aperture is composed of two crossed slots of different lengths to realize CP operation. However, this antenna exhibits very narrow CP bandwidth operation. Then, four identical inverted L-shaped patches are adopted as the loading parasitic components around the CP ME dipole antenna (proposed antenna) to enhance the CP bandwidth further. The effects of the parasitic inverted L-shaped shorted patches on the $|S_{11}|$ and ARs performance are studied, with simulated results shown in Figure 2(b). We kept the dimensions of the reference antenna and the proposed antenna the same for a fair comparison. As indicated in this figure, the reference antenna can realize a wide impedance bandwidth (for $|S_{11}| \leq -10$ dB) of 44.43% from 3.19 to 4.96 GHz. However, its 3 dB AR bandwidth is of only approximately 9.26% from 3.40 to 3.73 GHz. In contrast, when loading with the parasitic inverted L-shaped patches, both the impedance bandwidth and the 3 dB AR bandwidth are considerably expanded. The proposed antenna has a broad impedance bandwidth of approximately 51.82% from 3.16 to 5.37 GHz and a broad 3 dB AR bandwidth of 51.35% from 3.17 to 5.36 GHz, which falls entirely inside the impedance bandwidth. Clearly, an increase of approximately six times in the 3 dB AR bandwidth is achieved by simply loading the parasitic inverted L-shaped shorted patches. It is also concluded that the proposed antenna attains broad overlapping 3 dB AR/impedance bandwidth of 51.35% from 3.17 to 5.36 GHz.

To clarify the effect of parasitic inverted L-shaped shorted patches on the broadband CP operation, two orthogonal electric far-field components $|E_x|$ and $|E_y|$ observed in the broadside direction are investigated. Simulated results are depicted in Figure 2(c). As is commonly known, to generate CP waves, $|E_x|/|E_y| = 1$ and a phase difference ($PD = \angle E_x - \angle E_y$) of $\pm 90°$ should be achieved simultaneously [15]. As observed in Figure 2(c), although the reference antenna has a slowly varying magnitude ratio $|E_x|/|E_y|$ of around 1, it also shows considerable PD variation at its frequency of around 3.6 GHz. As a result, a narrow CP bandwidth is achieved in the reference antenna. Meanwhile, by loading with parasitic inverted L-shaped shorted patches, the proposed antenna exhibits a small amount of variation in both PD around $-90°$ and the magnitude ratio $|E_x|/|E_y|$ of around 1 against the frequency, hence achieving a much wider CP bandwidth. The induced current distribution on the parasitic inverted L-shaped patches at 4.5 GHz is studied and the simulated results are shown in Figure 3. The currents on the horizontal patches of the parasitic elements at $t = 0$ are orthogonal to that at $t = T/4$ and they rotate clockwise as time t increases. These induced currents are contributed to the far-field radiation of

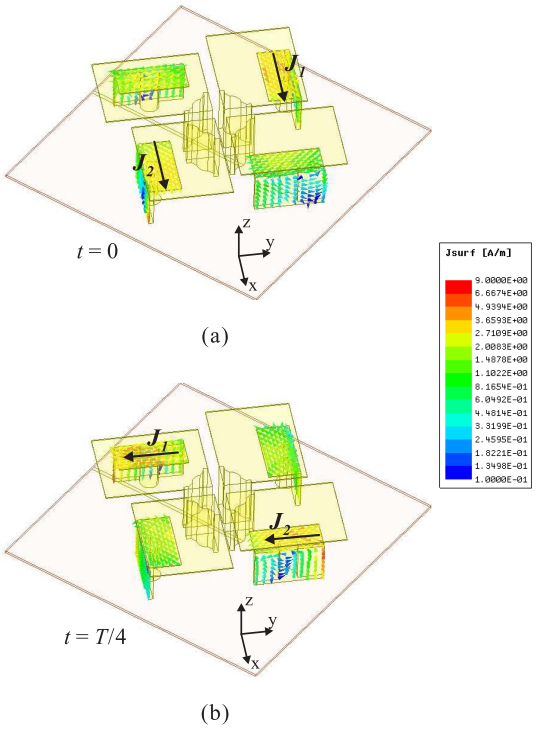

FIGURE 3. Simulated current distribution on four parasitic inverted L-shaped patches at 4.5 GHz. (a) $t = 0$. (b) $t = T/4$.

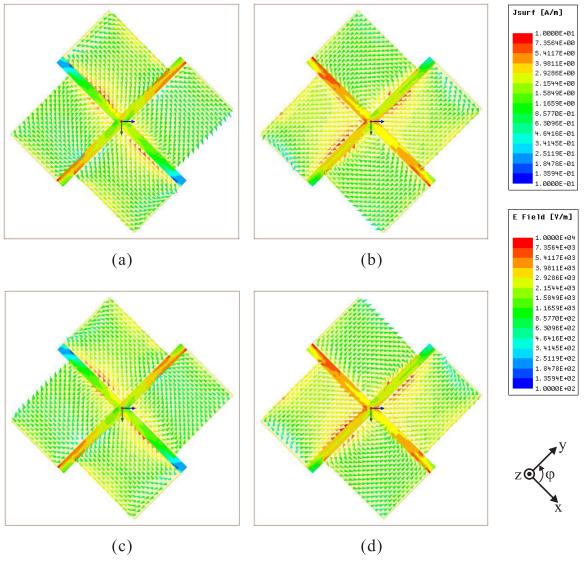

FIGURE 4. Simulated current distributions on the horizontal patches and electric field distributions on the aperture with period T for the proposed CP ME dipole antenna at 3.6 GHz. (a) $t = 0$. (b) $t = T/4$. (c) $t = T/2$. (d) $t = 3T/4$.

the proposed antenna, detuning the amplitude and phase of the $|E_x|$ and $|E_y|$ far-field components. This makes the $|E_x|$ and $|E_y|$ far-field components achieve a 90° phase difference and the same amplitude in a wide frequency band.

Simulated current on the horizontal patches and an electric field on the aperture at 3.60 GHz are investigated to explain the working principle of the proposed antenna. These results

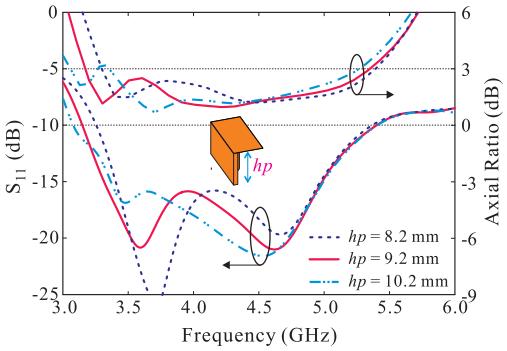

FIGURE 5. Simulated $|S_{11}|$ and ARs versus the frequency with different *hp* values.

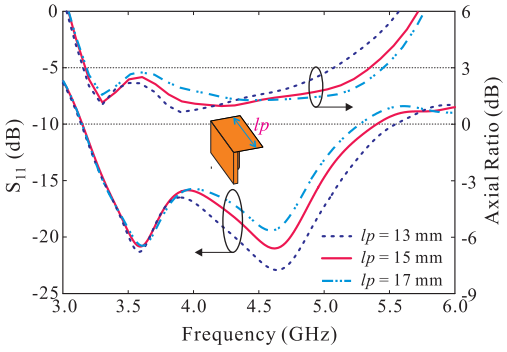

FIGURE 6. Simulated $|S_{11}|$ and ARs versus the frequency with different *lp* values.

are illustrated in Figure 4. At $t = 0$ and $T/2$, the electric dipole in the x-direction is excited as the currents on the horizontal patches are directed along the x-direction. Also, the electric field reaches its maximum across the portion of the radiating aperture along the y-direction, indicating that the magnetic dipole in the y-direction is excited simultaneously. On the other hand, at $t = T/4$ and $3T/4$, the electric dipole is excited mainly in the y-direction, while the magnetic dipole is excited strongly in the x-direction. Therefore, it is revealed that the simultaneously excited electric and magnetic dipoles in a crossed location can function as a complementary antenna [24]. Furthermore, the two sets of combinations that contribute to the radiation with orthogonal polarizations are excited with nearly equal amplitudes and a 90° phase difference (corresponding to a time delay of $T/4$), resulting in far-field CP radiation. As also observed in Figure 4, both the surface currents and electric fields rotate clockwise as the time t increases, indicating that the proposed antenna radiates LHCP waves.

C. PARAMETRIC STUDIES

For a better understanding of how the parasitic inverted L-shaped shorted patches affect the performance of the antenna, a parametric study is conducted. Certain critical parameters are chosen for the parametric study, including the height *hp*, the length *lp*, the width *wp*, and the

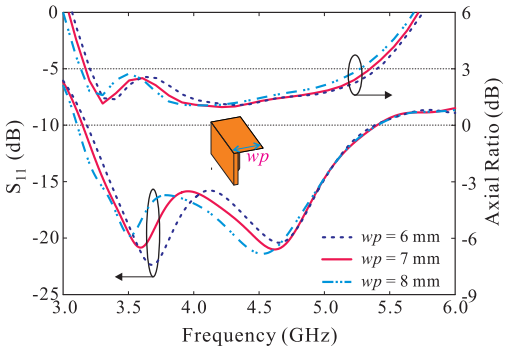

FIGURE 7. Simulated $|S_{11}|$ and ARs versus the frequency with different *wp* values.

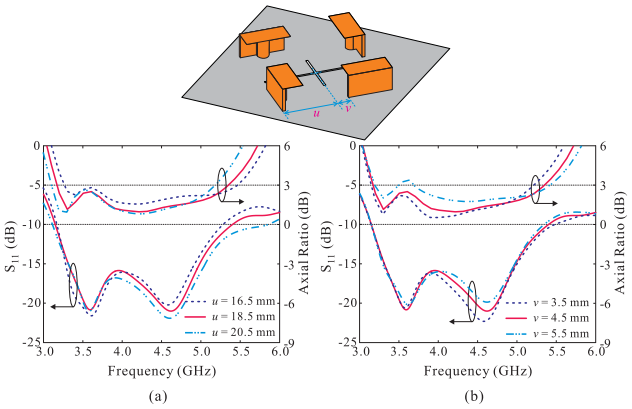

FIGURE 8. Simulated $|S_{11}|$ and ARs versus the frequency with different *u* and *v* values.

positions u and v of the parasitic inverted L-shaped shorted patches. As one parameter is investigated, the others are held constant at the optimum values listed in Table 1.

Figure 5 shows the effect of the height hp on the $|S_{11}|$ and the AR performance. As indicated in this figure, hp has a significant impact on the impedance matching and AR values at lower frequencies. The impedance and 3 dB AR bandwidths are expanded to a lower frequency range as hp increases. With $hp = 10.2$ mm, the AR exceeds 3 dB at around 3.3 GHz. Thus, $hp = 9.2$ mm is finally selected for the widest overlapping impedance/AR bandwidth.

Figure 6 demonstrates the effect of the length lp on the $|S_{11}|$ and the AR performance. As lp decreases, the impedance matching expands to a higher frequency range. However, the 3 dB AR bandwidth becomes narrower. Therefore, considering the tradeoff between the impedance bandwidth and the 3 dB AR bandwidth when varying lp, the value of lp is finally set to 15 mm.

Figure 7 depicts $|S_{11}|$ and the AR with different values of wp. As wp increases, the impedance matching slightly extends to lower frequencies. However, 3 dB AR bandwidth also shifts downwards to the lower frequency range. To achieve the widest overlapping impedance/AR bandwidth, the optimal value of wp is set to 7 mm.

The variations of $|S_{11}|$ and the AR with different values of u and v are illustrated in Figure 8. As observed in Figure 8(a), by increasing the value of u, the impedance bandwidth becomes wider. However, the dB AR bandwidth shifts downward to the lower frequency range. Meanwhile, v does not have much of an effect on the impedance matching, as shown in Figure 8(b). When increasing the value of v to 5.5 mm, the AR exceeds 3 dB at around 3.6 GHz. Therefore, to obtain the widest overlapping impedance/AR bandwidth, the values of u and v are set to 18.5 mm and 4.5 mm, respectively.

III. EXPERIMENTAL RESULTS AND DISCUSSION

A prototype of the proposed CP ME dipole antenna was built for verification. Figure 9(a) shows a photograph of the fabricated antenna. All of the horizontal planar patches are made of copper with a thickness of 0.2 mm, while the vertical plates

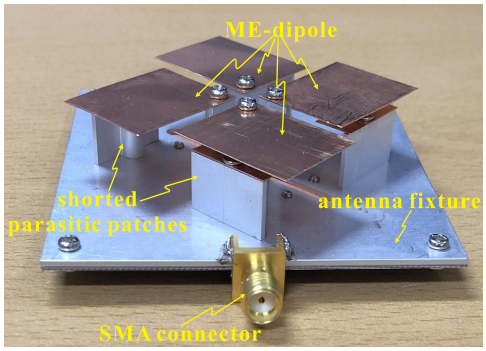

(a)

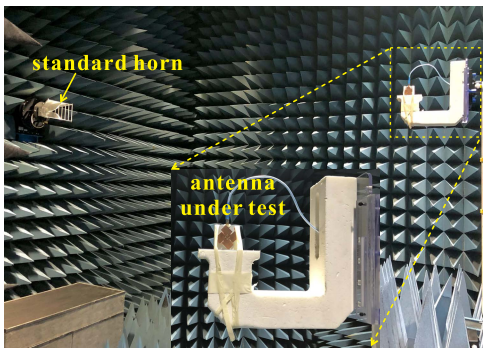

(b)

FIGURE 9. (a) Photograph of the fabricated antenna. (b) Measurement setup in an anechoic chamber.

are made of aluminum with a thickness of 1 mm. In order to ensure good mechanical strength, a square aluminum plate with a width of 65 mm and thickness of 1 mm is used as the antenna fixture to fix the vertical shorted plates and the substrate. To feed the ME dipole antenna conveniently, two crossed slots that are larger than the coupling slots on the ground, are also formed at the center of the square aluminum plate. The final structure is assembled and held in place with metal screws. The fabricated prototype is $65 \times 65 \times 12.7$ mm^3 in size. The $|S_{11}|$ property are examined with an

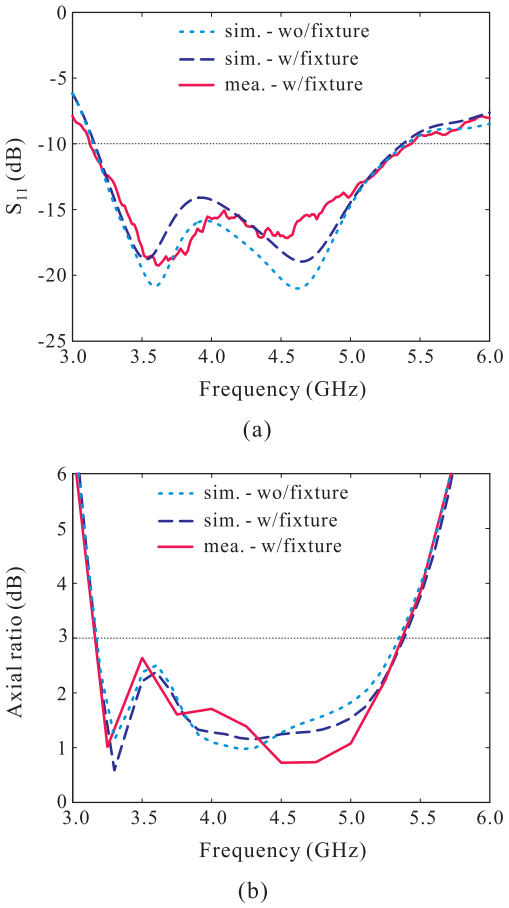

FIGURE 10. Simulated and measured of (a) $|S_{11}|$ and (b) ARs versus the frequency.

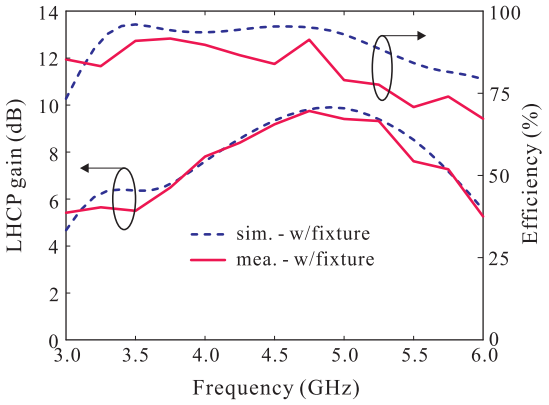

FIGURE 11. Simulated and measured of LHCP gains and total efficiencies versus the frequency.

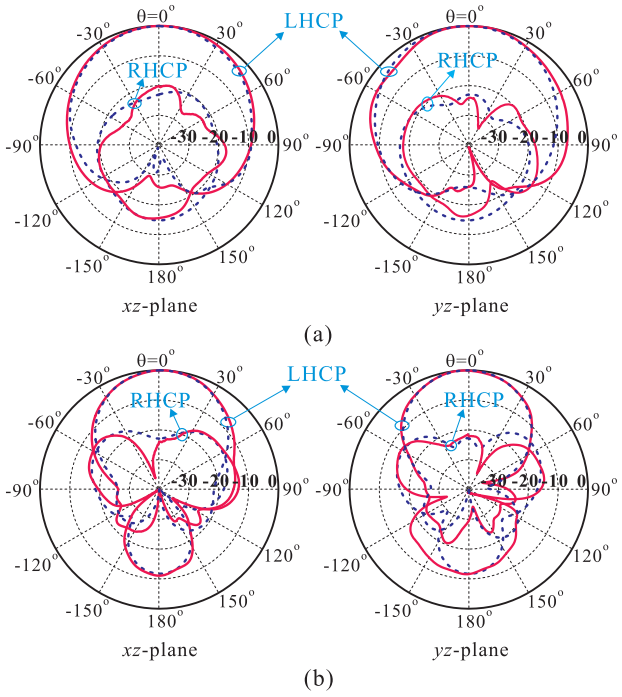

FIGURE 12. Simulated and measured normalized radiation patterns of the proposed CP ME dipole antenna at (a) 3.25 GHz and (b) 4.5 GHz (dotted lines are the simulated results and solid lines are the measured results).

Agilent 8510C RF vector network analyzer and the far-field properties are measured in a microwave anechoic chamber, as shown in Figure 9(b).

Figure 10 plots the measured results of $|S_{11}|$ and the ARs of the fabricated prototype. Simulated results of the proposed antenna with and without the antenna fixture are also included for comparison. As can be observed, the antenna fixture does not affect the antenna performance much. The measured impedance bandwidth ($|S_{11}| \leq -10$ dB) is 53.56% from 3.13 to 5.42 GHz (see Figure 10(a)). It can be seen in Figure 10(b) that the measured 3 dB AR bandwidth is 51.35% from 3.16 to 5.36 GHz, which is entirely covered by the measured impedance bandwidth. Figure 11 shows the simulated and measured results of the LHCP gains and total efficiencies. Within the 3 dB AR bandwidth, the measured LHCP gain is from 5.50 to 9.75 dBic. The corresponding simulated LHCP gain is from 6.30 to 9.90 dBic. The average measured efficiency of the antenna is approximately 85.99% across the 3 dB AR band, with a peak value of 91.27% at 4.75 GHz.

Figure 12 plots the measured and simulated normalized radiation patterns on the xz-plane ($\phi = 0°$) and yz-plane ($\phi = 90°$) at the frequencies of 3.25 GHz and 4.5 GHz. It is evident that the proposed antenna is an LHCP antenna, and that the radiation patterns are directional toward the $+z$-direction. On both planes for these two frequencies, the LHCP gains are approximately 22.5 dB more than the right-handed circular polarization (RHCP) gains in the $+z$-direction. Also, nearly identical radiation patterns are achieved on the xz-plane and yz-plane. In addition, the proposed antenna still exhibits a large RHCP in the $-z$-direction, especially at the higher frequencies. This is because the antenna is excited through a crossed slot, and the slot mode becomes stronger as the frequency increasing [22]–[24]. Due to the bidirectional radiation pattern property, the crossed slot exhibits the LHCP radiation in the $+z$-direction, which

TABLE 2. Comparison of the proposed low-profile CP ME dipole antenna and existing designs.

Ref.	Feeding Method	CP Bandwidth* [%]	Profile [λ_L]	Peak Gain [dBic]
[17]	Γ-shaped probe	41	0.24	6.3
[18]	Γ-shaped probe	79.7	0.16	10.6
[19]	Γ-shaped probe	67.5	0.177	10.4
[20]	aperture coupled	22.5	0.287	9.24
[21]	aperture coupled	23.5	0.166	8.4
[22]	aperture coupled	64.5	0.168	10.2
[23]	aperture coupled	12.8	0.122	7.8
This work	aperture coupled	51.35	0.134	9.75

λ_L is the wavelength at the lowest frequency of the CP band in free space.
*CP Bandwidth is the overlapping 3 dB AR/impedance bandwidth.

contributes to the LCHP radiation of the ME dipole antenna. Meanwhile, it also produces the RHCP radiation in the $-z$-direction, resulting in large back radiation. It is possible to override this drawback by placing the proposed antenna over an electromagnetic band gap surface [20]. In general, good agreement is noted between the simulation and measurement results. The slight deviation is mainly attributed to fabrication tolerance and measurement errors.

To highlight the advantages of the proposed antenna, we summarize the results of a comparison of our design and other reported CP ME dipole antennas in Table 2. Compared to previous CP ME dipole antennas ([17], [20], and [21]), the proposed antenna exhibits a wider CP bandwidth and a higher gain while maintaining a very low profile of only $0.134\lambda_L$. Although three earlier antennas ([18], [19], and [22]) have a wider CP bandwidth and a slightly higher gain their profiles are quite high. Compared to one design [23], the proposed antenna provides a much wider 3 dB AR bandwidth and a much higher gain.

IV. CONCLUSION

A low-profile and broadband cross-slot-coupled CP ME dipole antenna was presented in this paper. By adopting four identical inverted L-shaped patches as parasitic loading components around the ME dipole, a significant CP bandwidth enhancement was achieved. In order to verify the proposed design, an antenna prototype was fabricated and examined. The experimental results demonstrated a -10 dB reflection bandwidth of 53.57% from 3.13 to 5.42 GHz, a 3dB AR bandwidth of 51.35% from 3.16 to 5.36 GHz, a LHCP gain from 5.50 to 9.75 dBic, and nearly identical radiation patterns on two principle cutting planes across the operating band. Moreover, the antenna has a low profile of only $0.134\lambda_L$. Owing to these excellent features, the proposed antenna is a feasible candidate for satellite communication systems that operate on the C-band and for sub-6GHz 5G communications, among others.

REFERENCES

[1] K.-M. Luk and H. Wong, "A new wideband unidirectional antenna element," *Int. J. Microw. Opt. Technol.*, vol. 1, no. 1, pp. 35–44, Jul. 2006.
[2] L. Ge and K. M. Luk, "A wideband magneto-electric dipole antenna," *IEEE Trans. Antennas Propag.*, vol. 60, no. 11, pp. 4987–4991, Nov. 2012.
[3] K. M. Luk and B. Wu, "The magnetoelectric dipole—A wideband antenna for base stations in mobile communications," *Proc. IEEE*, vol. 100, no. 7, pp. 2297–2307, Apr. 2013.
[4] G. Yang, S. Zhang, J. Li, Y. Zhang, and G. Pedersen, "A multi-band magneto-electric dipole antenna with wide beam-width," *IEEE Access*, vol. 8, pp. 68820–68827, 2020.
[5] B. Feng, J. Lai, Q. Zeng, and K. Chung, "A dual-wideband and high gain magneto-electric dipole antenna and its 3D MIMO system with metasurface for 5G/WiMAX/WLAN/X-band applications," *IEEE Access*, vol. 6, pp. 33387–33398, 2018.
[6] C. Ding and K. M. Luk, "Low-profile magneto-electric dipole antenna," *IEEE Antennas Wireless Propag. Lett.*, vol. 15, pp. 1642–1644, 2016.
[7] Y. Li and K.-M. Luk, "A linearly polarized magnetoelectric dipole with wide H-plane beamwidth," *IEEE Trans. Antennas Propag.*, vol. 62, no. 4, pp. 1830–1836, Apr. 2014.
[8] Z. Wei, Z. Zhou, Z. Tang, J. Y. Yin, J. Ren, and Y. Yin, "Broadband filtering magnetoelectronic dipole antenna with quasi-elliptic gain response," *IEEE Trans. Antennas Propag.*, vol. 68, no. 4, pp. 3225–3230, Apr. 2020.
[9] L. Siu, H. Wong, and K. M. Luk, "A dual-polarized magneto-electric dipole with dielectric loading," *IEEE Trans. Antennas Propag.*, vol. 57, no. 3, pp. 616–623, Mar. 2009.
[10] S. J. Yang, Y. M. Pan, Y. Zhang, Y. Gao, and X. Y. Zhang, "Low-profile dual-polarized filtering magneto-electric dipole antenna for 5G applications," *IEEE Trans. Antennas Propag.*, vol. 67, no. 10, pp. 6235–6243, Oct. 2019.
[11] W. Cao, Q. Wang, Z. Qian, S. Shi, and J. Jin, "Gain enhancement for wideband CP ME-dipole antenna by loading with spiral strip in Ku-band," *IEEE Trans. Antennas Propag.*, vol. 66, no. 2, pp. 962–966, Feb. 2018.
[12] S. Trinh-Van, T. Van Trinh, Y. Yang, K.-Y. Lee, and K. C. Hwang, "A broadband circularly polarized magneto-electric dipole array antenna for 5G millimeter-wave applications," *Appl. Phys. Lett.*, vol. 119, no. 2, Jul. 2021, Art. no. 023503.
[13] J. Xu, W. Hong, Z. H. Jiang, and H. Zhang, "Low-cost millimeter-wave circularly polarized planar integrated magneto-electric dipole and its arrays with low-profile feeding structures," *IEEE Antennas Wireless Propag. Lett.*, vol. 19, no. 8, pp. 1400–1404, Aug. 2020.
[14] Y. Li and K.-M. Luk, "A 60-GHz wideband circularly polarized aperture-coupled magneto-electric dipole antenna array," *IEEE Trans. Antennas Propag.*, vol. 64, no. 4, pp. 1325–1333, Apr. 2016.
[15] S. Gao, Q. Luo, and F. Zhu, *Circularly Polarized Antennas*. West Sussex, U.K.: Wiley, 2014.
[16] U. Banerjee, A. Karmakar, and A. Saha, "A review on circularly polarized antennas, trends and advances," *Int. J. Microw. Wireless Technol.*, vol. 12, no. 9, pp. 922–943, Nov. 2020.
[17] P. Mohammadi, M. Rezvani, and T. Siahy, "A circularly polarized wideband magneto-electric dipole antenna with simple structure for BTS applications," *AEU-Int. J. Electron. Commun.*, vol. 105, pp. 92–97, Jun. 2019.
[18] C.-Q. Feng, F.-S. Zhang, H.-J. Zhang, and J.-X. Su, "A single-feed circularly polarized magnetoelectric dipole antenna for wideband wireless applications," *Prog. Electromagn. Res. M*, vol. 65, pp. 1–8, 2018.
[19] M. Han and W. Dou, "Low profile broadband circularly polarized magnetoelectric dipole antenna with short-circuit patch for wireless communication," *Microw. Opt. Technol. Lett.*, vol. 62, pp. 1307–1314, 2020.
[20] J. Sun and K.-M. Luk, "Wideband linearly-polarized and circularly-polarized aperture-coupled magneto-electric dipole antennas fed by microstrip line with electromagnetic bandgap surface," *IEEE Access*, vol. 7, pp. 43084–43091, 2019.

[21] K. Sun, D. Q. Yang, and S. H. Liu, "A wideband hybrid feeding circularly polarized magneto-electric dipole antenna for 5G Wi-Fi," *Microw. Opt. Technol. Lett.*, vol. 60, no. 8, pp. 1837–1842, Aug. 2018.
[22] X. Cui, F. Yang, and M. Gao, "Wideband CP magnetoelectric dipole antenna with microstrip line aperture-coupled excitation," *Electron. Lett.*, vol. 57, no. 14, pp. 863–864, 2018.
[23] S. Wu, J. Zhao, and J. Xu, "A circularly polarized low-profile magnetoelectric dipole antenna," *Microw. Opt. Technol. Lett.*, vol. 63, no. 11, pp. 2852–2858, 2021.
[24] X. Cui, F. Yang, M. Gao, L. Zhou, Z. Liang, and F. Yan, "A wideband magnetoelectric dipole antenna with microstrip line aperture-coupled excitation," *IEEE Trans. Antennas Propag.*, vol. 65, no. 12, pp. 7350–7354, Dec. 2017.

SON TRINH-VAN was born in Hanoi, Vietnam, in 1986. He received the B.Sc. (Eng.) degree in electronics and telecommunications from the Hanoi University of Science and Technology, Hanoi, in 2010, and the Ph.D. degree from the Division of Electronics and Electrical Engineering, Dongguk University, Seoul, South Korea, in 2015. He is currently a Research Professor with the Department of Electrical and Computer Engineering, Sungkyunkwan University, Suwon, South Korea. His research interests include design of circularly polarized antennas and millimeter-wave antennas and arrays.

YOUNGOO YANG (Senior Member, IEEE) was born in Hamyang, South Korea, in 1969. He received the Ph.D. degree in electrical and electronic engineering from the Pohang University of Science and Technology (Postech), Pohang, South Korea, in 2002. From 2002 to 2005, he was with Skyworks Solutions Inc., Newbury Park, CA, USA, where he designed power amplifiers for various cellular handsets. Since March 2005, he has been with the School of Information and Communication Engineering, Sungkyunkwan University, Suwon, South Korea, where he is currently a Professor. His research interests include RF/mm-wave power amplifiers, RF transmitters, and DC–DC converters.

KANG-YOON LEE (Senior Member, IEEE) received the B.S., M.S., and Ph.D. degrees from the School of Electrical Engineering, Seoul National University, Seoul, South Korea, in 1996, 1998, and 2003, respectively. From 2003 to 2005, he was with GCT Semiconductor Inc., San Jose, CA, USA, where he was a Manager of the Analog Division and worked on the design of CMOS frequency synthesizer for CDMA/PCS/PDC and single-chip CMOS RF chip sets for W-CDMA, WLAN, and PHS. From 2005 to 2011, he was an Associate Professor with the Department of Electronics Engineering, Konkuk University. Since 2012, he has been with the School of Information and Communication Engineering, Sungkyunkwan University, where he is currently an Associate Professor. His research interests include implementation of power integrated circuits, CMOS RF transceiver, analog integrated circuits, and analog/digital mixed-mode VLSI system design.

KEUM CHEOL HWANG (Senior Member, IEEE) received the B.S. degree in electronics engineering from Pusan National University, Busan, South Korea, in 2001, and the M.S. and Ph.D. degrees in electrical and electronic engineering from the Korea Advanced Institute of Science and Technology (KAIST), Daejeon, South Korea, in 2003 and 2006, respectively.

From 2006 to 2008, he was with Samsung Thales, Yongin, South Korea, where he was involved with the development of various antennas for wireless communication and radar systems. From 2008 to 2014, he was an Associate Professor with the Division of Electronics and Electrical Engineering, Dongguk University, Seoul, South Korea. In 2015, he joined the Department of Electrical and Computer Engineering, Sungkyunkwan University, Suwon, South Korea, where he is currently a Professor. His research interests include advanced electromagnetic scattering and radiation theory and applications, design of multi-band/broadband array antennas, and optimization algorithms for electromagnetic applications.

Prof. Hwang is a Life Member of KIEES and a member of IEICE.